

# Star-disk interactions in T Tauri star V2129 Oph: combining optical and infrared spectroscopy

A. P. Sousa<sup>1</sup>, J. Bouvier<sup>1</sup>, S. H. P. Alencar<sup>2</sup>, J.-F. Donati<sup>3</sup>, E. Alecian<sup>1</sup>, and the SPIRou consortium

<sup>1</sup>Institut de Planétologie et d'Astrophysique de Grenoble - IPAG - France

<sup>2</sup>Universidade Federal de Minas Gerais - UFMG - Brasil

<sup>3</sup>Univ. de Toulouse - France

alana.sousa@univ-grenoble-alpes.fr

## 1 Introduction

Low mass accreting stars are known as classical T Tauri stars (CTTSs) and are characterized by emission lines e.g.  $H\alpha$ ,  $H\beta$ , He (Bouvier et al., 2020; Alencar et al., 2018; Sousa et al., 2016; Costigan et al., 2012; Kwan & Fischer, 2011; Fang et al., 2009) that vary in intensity and morphology as the star-disk system rotates (Fig. 1).

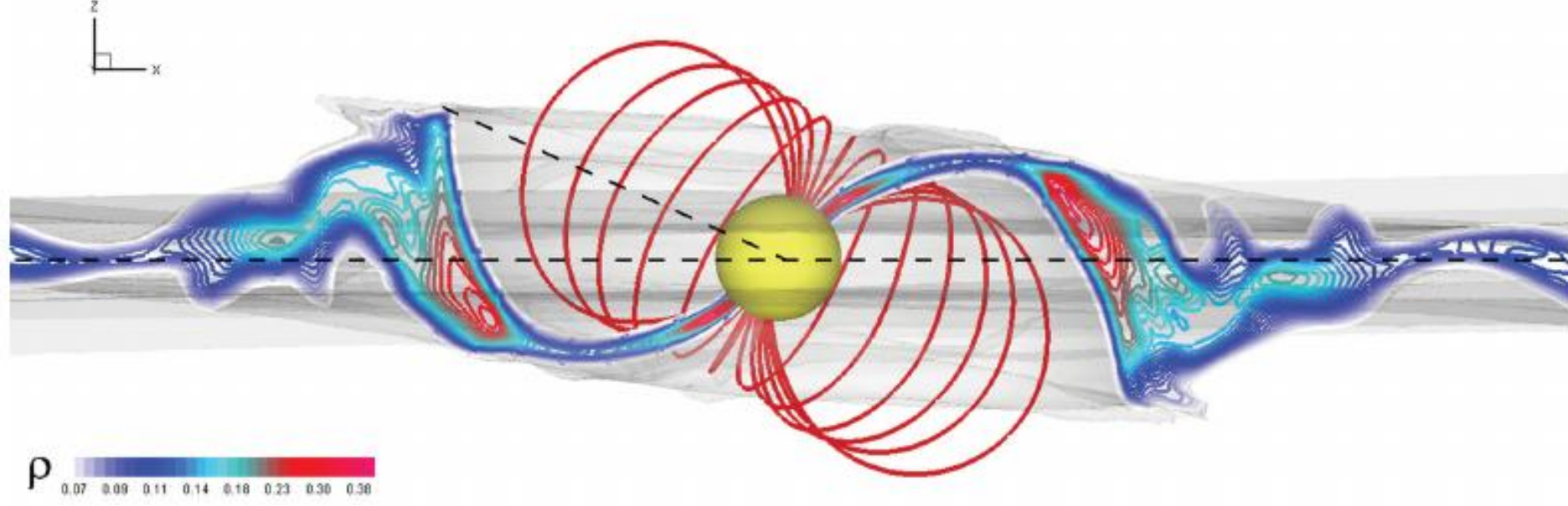


**Figure 1.** MHD simulation of accretion onto a CTTS. This simulation shows the accreting funnel existing due to the inclination between of the magnetic field axis and the rotational axis of the star (Romanova et al., 2013). Red lines show selected magnetic field lines.

V2129 Oph (SR9, DoAr 34, AS 207, ROX 29) is well-known young star ( $1 - 2 \text{ Myr}$ ) with K5 spectral type (Torres et al., 2006), located in the  $\rho$  Oph star forming region, at a distance of  $130 \pm 1 \text{ pc}$  (Bailer-Jones et al., 2018). V2129 Oph accretes at a moderate rate of  $(1.5 \pm 0.6) \times 10^{-9} M_{\odot}$  from its circumstellar disk (Alencar et al., 2012) and we view the system at a inclination of about  $\sim 60^\circ$  from our line of sight (Donati et al., 2011). We adopt (and confirm) the rotational period of 6.53 days derived initially using photometric data (Shevchenko & Herbst, 1998), and confirmed spectroscopically from spot-modulated radial velocity variations (Alencar et al., 2012).

Donati et al. (2007) & Donati et al. (2011) measured an increase in the magnitude of the dipole and the octupole magnetic field components over a timescale of few years. A change in the magnetic field's intensity can significantly impact the star's accretion properties. In this work, we analyze the accretion/ejection process in V2129 Oph through the variability of the circumstellar emission lines, and compare our results with previous works to investigate the dynamics of the system on a timescale of a decade.

## 2 Observation

- 10 observations in the optical with CFHT/ESPaDOnS spectrograph (20-jun to 04-jul 2018)
- 9 observations in the optical with ESO/HARPS spectrograph (29-jun to 14-jul 2018)
- 9 observations in the near-infrared with CFHT/SPIRou spectrograph (25-Jul to 06-Aug 2018)

## 3 Optical and near-infrared radial velocities and veiling

We computed the optical and IR radial velocities using ESPaDOnS, HARPS and SPIRou data independently, see Fig. 2. We find the radial velocity to be rotationally modulated by two sets of cold spots located at nearly opposite longitudes at the stellar surface, or an elongated polar spot with latitudinal extensions at opposite azimuths.

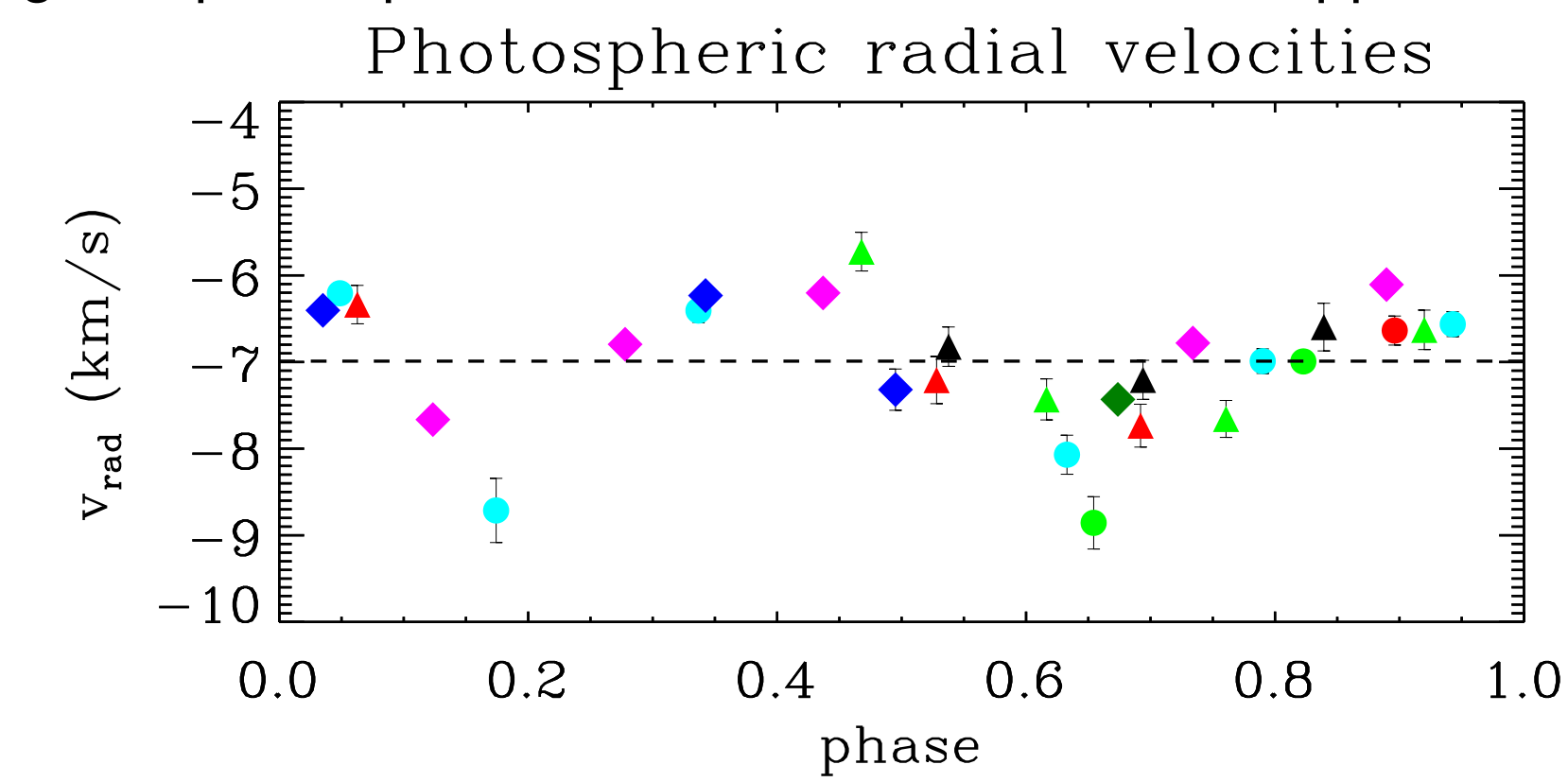


**Figure 2.** Radial velocity of photospheric lines measured with ESPaDOnS (triangles), HARPS (circles) and SPIRou (diamonds) spectra and plotted in phase with the ephemeris from Alencar et al. (2012) & Donati et al. (2007). The colors represent different cycles. The shape of the optical and IR radial velocity variations is similar. The amplitude of IR the radial velocity curve appears about two times smaller than the amplitude of the optical one, though SPIRou measurements are lacking towards the radial velocity minimum.

To measure the rotation phases (E), we used the same ephemeris adopted by Alencar et al. (2012) and Donati et al. (2007):

$$HJD = 2453540.0 + P_{\text{rot}}E, \quad (1)$$

where  $P_{\text{rot}} = 6.53 \text{ days}$  is the stellar rotational period.

We also derived the wavelength-dependent veiling across the optical (Fig. 3) and near infrared ranges (Fig. 4).

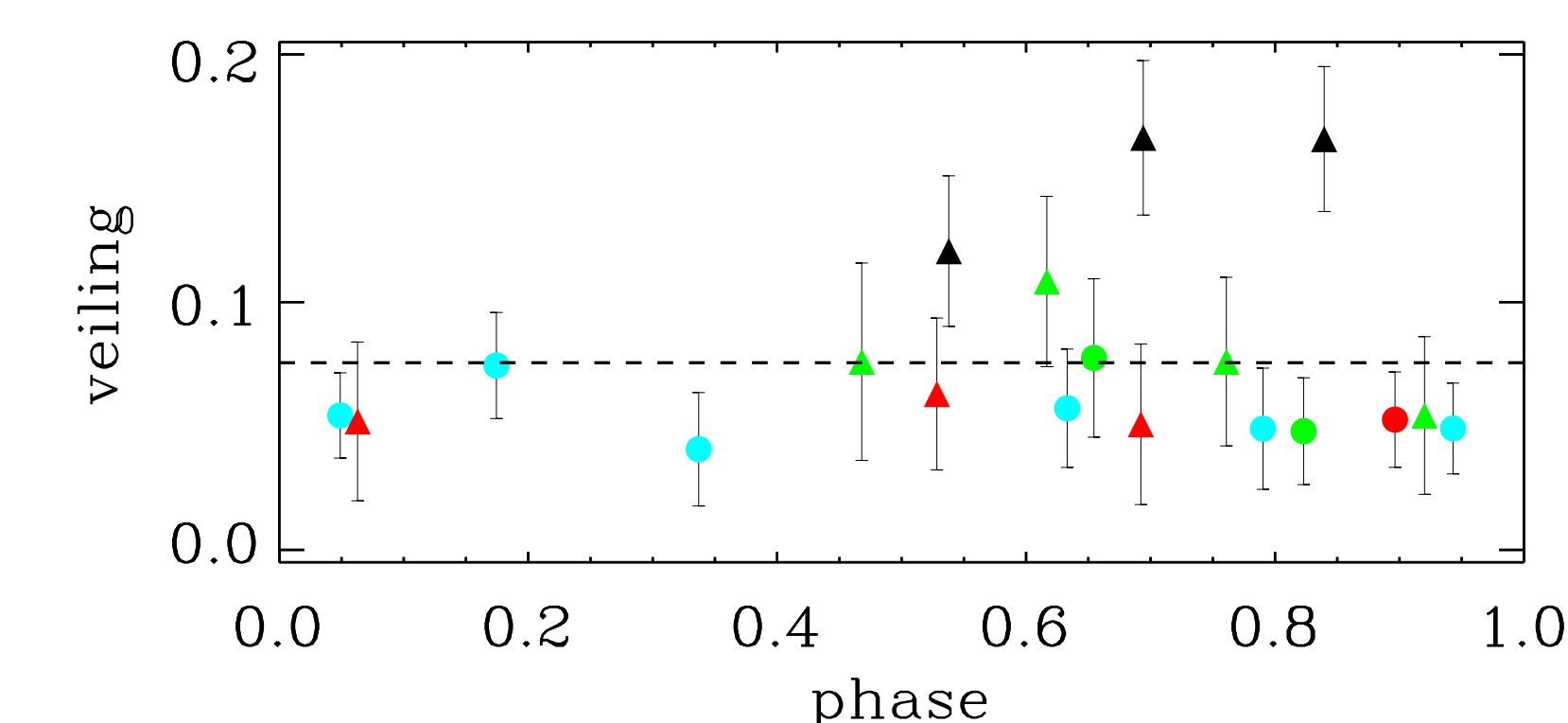


**Figure 3.** Optical veiling of photospheric lines as a function of the stellar rotation phase. The optical veiling corresponds to mean values obtained from all spectroscopic regions used in the calculations. The error bars come from the standard deviations. The colors represent different cycles.

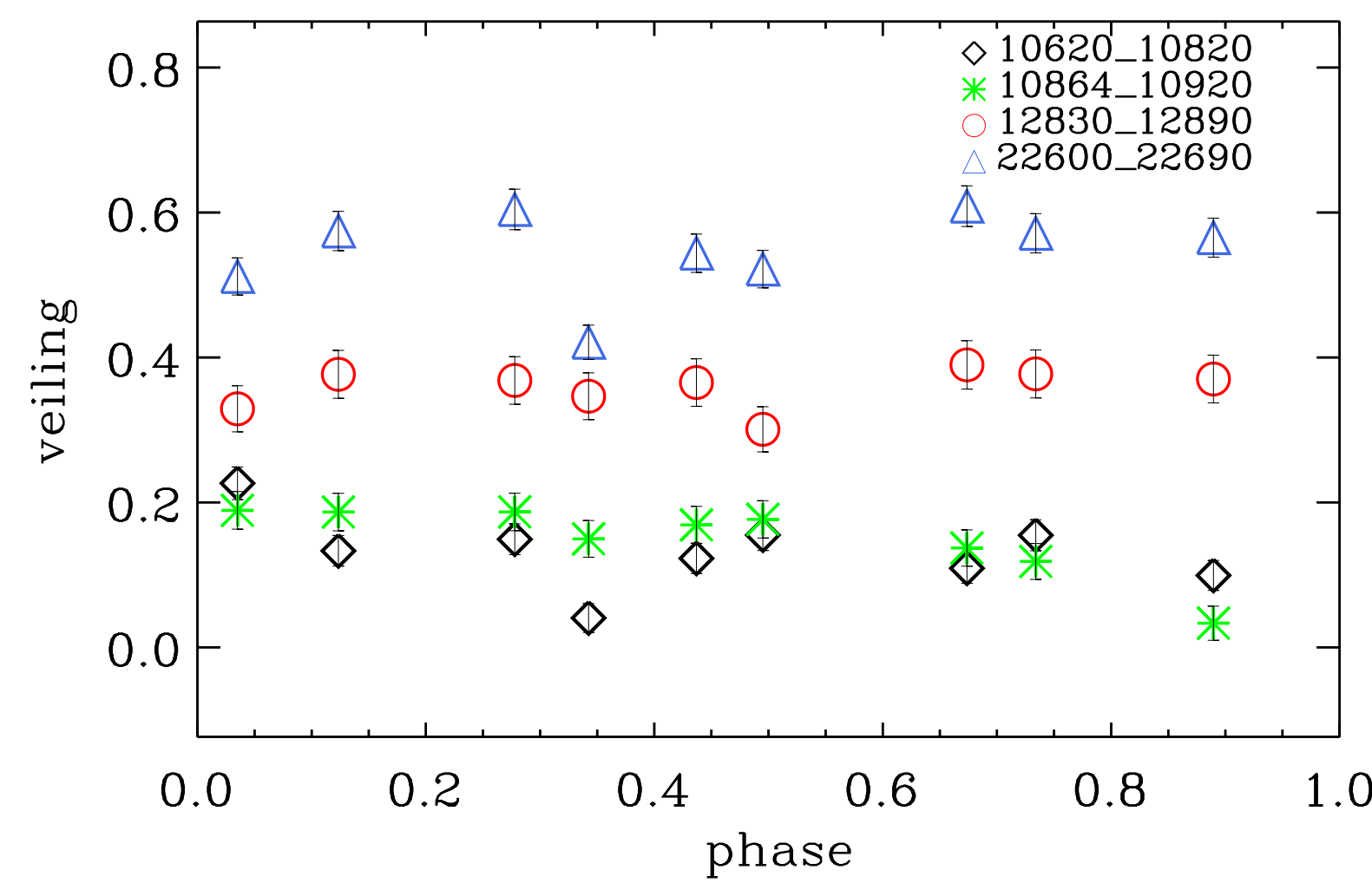


**Figure 4.** Veiling of photospheric lines obtained with SPIRou data as a function of the stellar rotation phase. Each symbol shows the veiling measured in different spectral regions.

## 4 Optical and near-infrared emission lines

The emission lines of V2129 Oph (Fig. 5) are broad, intense and variable from night to night, which are characteristics of accreting system. The Balmer lines and the infrared HeI line present redshifted absorptions below the continuum at some rotational phases, commonly associated with the passage of the accretion funnel across our line of sight. The HeI (10830 Å) also presents a blueshifted absorption component persistent in all phases, which varies in depth and width as the system rotates. Usually, the blueshifted absorptions are characteristic of ejection processes, as a disk or stellar wind (Edwards et al., 2006).

In the NaI line of V2129 Oph, we see at least two blueshifted absorption components located around  $-40$  and  $-80 \text{ km s}^{-1}$ , among other higher velocity components ( $< -100 \text{ km s}^{-1}$ ) that appear only at some nights, and may represent transient outflows.

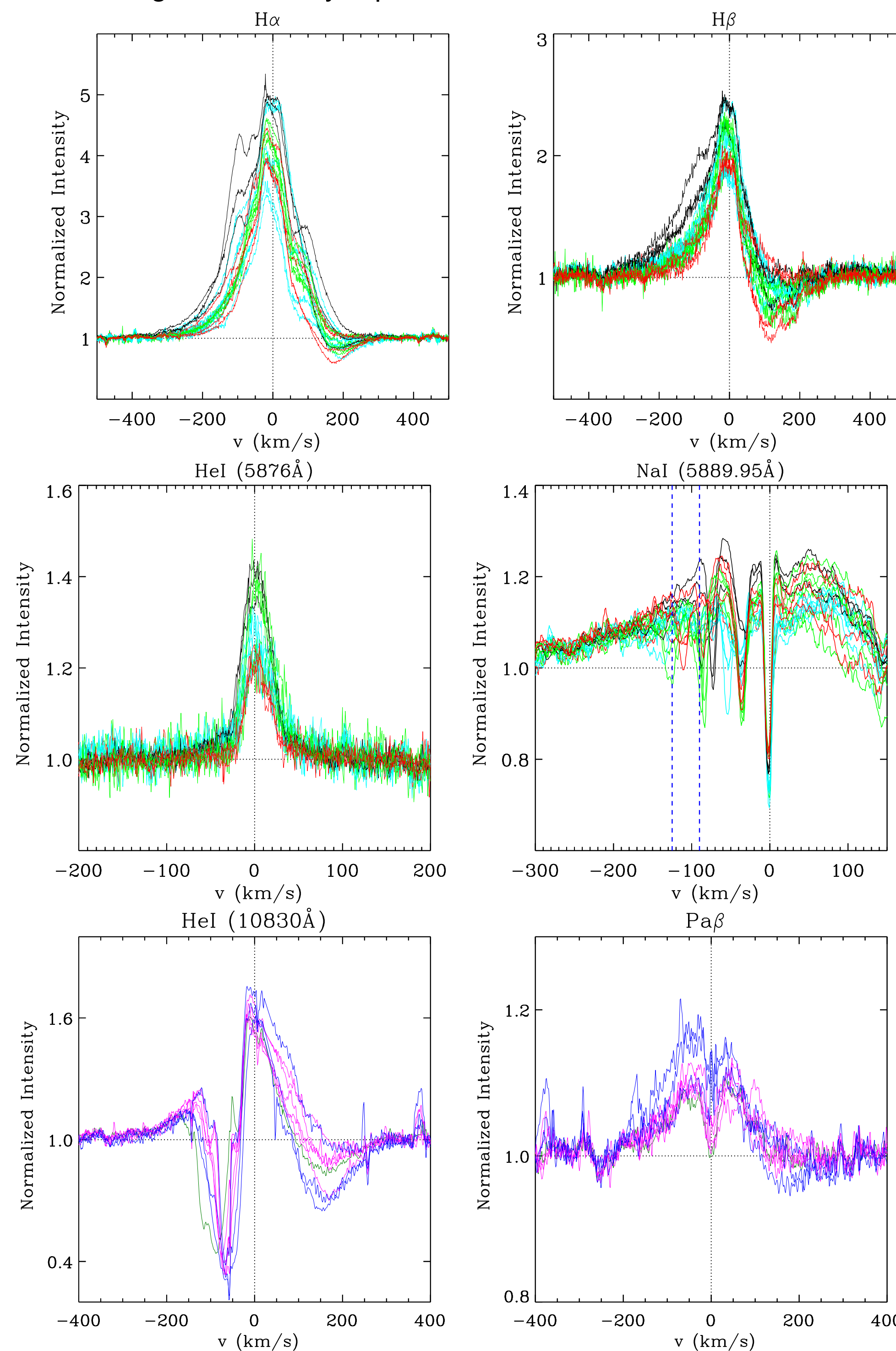


**Figure 5.** The line profiles, obtained with the ESPaDOnS, HARPS and SPIRou spectrographs, colors correspond to different rotation cycles. The two blue vertical lines delimit the periodic region of Na I line.

In the table below we show observational parameters measured in the V2129 Oph optical and infrared spectra.

Parameter	Value obtained
Rotation period	6.53 days
Period $H\alpha$	8.5 days
Period HeI (5876 Å)	6.0 days
Period $H\beta$	6.0 days/ 8.5 days
Period NaI (5889.95 Å)	9.0 days
Period HeI (10830 Å)	6.0 days
Period Pa $\beta$	6.0 days
$V_{\text{rad}}$	$-7.1 \pm 0.8 \text{ km s}^{-1}$
$EW_{H\alpha}$	$11.5 \pm 3.3 \text{ Å}$
$EW_{H\beta}$	$2 \pm 1 \text{ Å}$
$EW_{HeI(5876 \text{ Å})}$	$0.27 \pm 0.08 \text{ Å}$
$EW_{NaIDoublet}$	$1.3 \pm 0.4 \text{ Å}$
$EW_{HeI(10830 \text{ Å})}$	$1.1 \pm 1.3 \text{ Å}$
$EW_{Pa\beta}$	$0.9 \pm 0.3 \text{ Å}$
$\dot{M}_{HeI(5876 \text{ Å})}$	$(1.5 \pm 0.5) \times 10^{-9} M_{\odot} \text{ yr}^{-1}$

## 5 Circumstellar lines periodicity

We applied a Lomb-Scargle periodogram analysis to all emission lines and, surprisingly, different lines exhibit different periodicities and sometimes even a varying period across the line profile. A period of 6.0 days, shorter than the 6.53 days rotational period, is measured in the HeI 5876 Å line profile. Conversely, a longer period of 8.5 days is measured in the  $H\alpha$  and in the red wing of the  $H\beta$  profiles. The longer period suggests the emission arises from a structure located beyond the disk corotation radius. While the origin of the multiple periods seen in the line profiles remains puzzling. Various possibilities for the circumstellar configuration, including a trailing funnel flow, multiple accretion flows, or an external disturbance, can be responsible for this period, see Sousa et al. (Submitted).

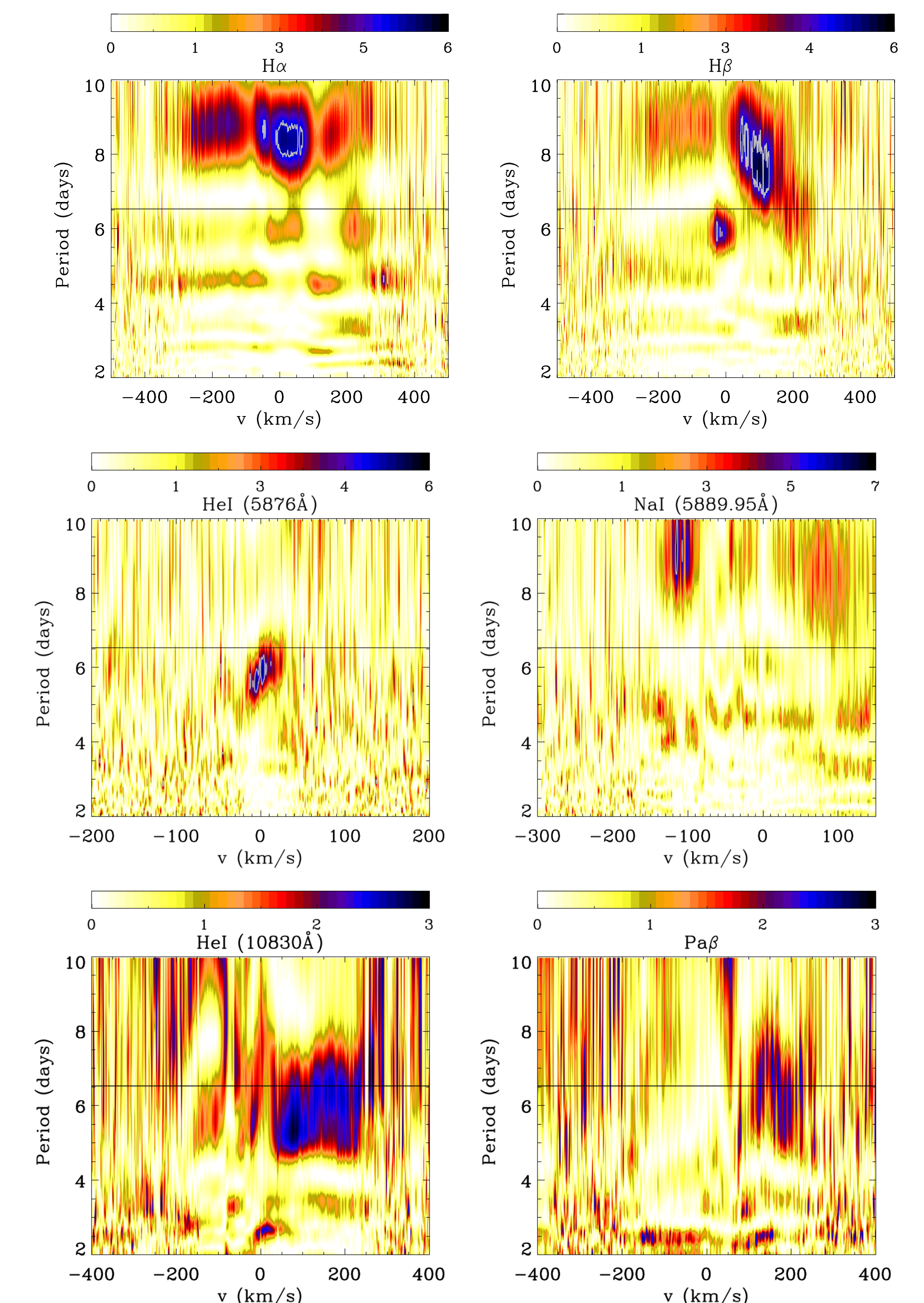


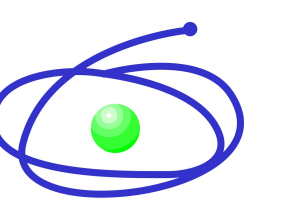
**Figure 6.** Bi-dimensional periodograms of the optical and infrared circumstellar lines. The color range corresponds to the power of the periodogram and the horizontal line represents the star's rotation period,  $P = 6.53 \text{ days}$ . The white contour represents the false alarm probability level of about 95% of confidence.

In previous works, the variability of the circumstellar lines of V2129 Oph can be explained by stable magnetospheric accretion, even taking into account the complexity of its surface magnetic field. Indeed, except for the central part of the  $H\alpha$  line, most line profile variability was modulated on a period consistent with the 6.53 days rotational period of the central star, as expected if the magnetosphere truncates the disk close to the corotation radius Alencar et al. (2012). This indicates that the dynamics of the accretion/ejection process can significantly vary on a timescale of just a few years in this source, presumably reflecting the evolving magnetic field topology at the stellar surface.

## 6 Conclusions

The combination of quasi-simultaneous optical and near infrared spectroscopy allows for a detailed characterization of the system's properties and variability. Comparing our results to those obtained from previous campaigns performed on V2129 Oph over the last 12 years, we find that the mass accretion rate onto the star hardly varied and both the shape and intensity of the emission line profiles remained fairly stable over this timescale. However, the variability pattern of the lines changed drastically, with new periodicities appearing that were either not seen or were not dominant during previous monitoring campaigns. Our data provide further evidence that the environment of classical T Tauri stars can be very dynamic on a timescale of a few years and suggest that the topology of their surface magnetic field may significantly evolve over this timescale.

## 7 Acknowledgments



## References

- Alencar, S. H. P., Bouvier, J., Donati, J.-F., et al. 2018, *A&A*, 620, A195
- Alencar, S. H. P., Bouvier, J., Walter, F. M., et al. 2012, *A&A*, 541, A116
- Bailer-Jones, C. A. L., Rybizki, J., Fournesneau, M., Mantelet, G., & Andrae, R. 2018, *AJ*, 156, 58
- Bouvier, J., Alecian, E., Alencar, S. H. P., et al. 2020, *A&A*, 643, A99
- Costigan, G., Scholz, A., Stelzer, B., et al. 2012, *MNRAS*, 427, 1344
- Donati, J., Jardine, M. M., Gregory, S. G., et al. 2007, *MNRAS*, 380, 1297
- Donati, J.-F., Bouvier, J., Walter, F. M., et al. 2011, *MNRAS*, 412, 2454
- Edwards, S., Fischer, W., Hillenbrand, L., & Kwan, J. 2006, *ApJ*, 646, 319
- Fang, M., van Boekel, R., Wang, W., et al. 2009, *A&A*, 504, 461
- Kwan, J. & Fischer, W. 2011, *MNRAS*, 411, 2383
- Romanova, M. M., Ustyugova, G. V., Koldoba, A. V., & Lovelace, R. V. E. 2013, *MNRAS*, 430, 699
- Shevchenko, V. S. & Herbst, W. 1998, *AJ*, 116, 1419
- Sousa, A. P., Alencar, S. H. P., Bouvier, J., et al. 2016, *A&A*, 586, A47
- Torres, C. A. O., Quast, G. R., da Silva, L., et al. 2006, *A&A*, 460, 695